International Forum on Aeroelasticity and Structural Dynamics
IFASD 2019
9-13 June 2019, Savannah, Georgia, USA

NUMERICAL ANALYSIS OF LIMIT CYCLE OSCILLATION OF A SUPERSONIC TRANSPORT WIND TUNNEL TEST MODEL

Kenichi SAITOH[1], Hamidreza KHEIRANDISH[2] and Norio YOSHIMOTO[3]

[1, 3] Japan Aerospace Exploration Agency
6-13-1, Osawa, Mitaka, Tokyo, 181-0015, Japan
kenichi.saitoh@jaxa.jp
norio.yoshimoto@jaxa.jp

[2] Advanced Science & Intelligence Research Institute
1-18-14, Uchikanda, Chiyoda-ku, Tokyo, 101-0047, Japan
hamidkh@asiri.co.jp

Keywords: Super Sonic Transport, transonic speed, LCO, Euler analysis, Harmonic balance method.

Abstract: In the previous experimental research of aeroelasticity for supersonic transport wing model, limit cycle oscillation (LCO) boundary and amplitude characteristics have been obtained. The LCO started from smaller amplitude and grew up suddenly as dynamic pressure increased. Numerical analysis was performed for it, and large amplitude LCO was captured by Euler simulation. Bifurcation diagram was obtained by Harmonic balance method, and LCO amplitude is estimated.

1 INTRODUCTION

Transonic is a critical region in aeroelasticity even for a supersonic transport (SST). Furthermore, for the wing which is thin and low aspect ratio, a special characteristics such as instability in very narrow Mach range so called “chimney”[1] and divergent flutter at higher dynamic pressure than LCO region[2] have been reported. Using fundamental wind tunnel aeroelastic model of SST, further investigation was performed by the authors[3]. In the experiment, LCO which has the bottom of dip at Mach 0.94 and 1.01 was observed. Large amplitude LCO was observed over the smaller amplitude LCO dynamic pressure area instead of the divergent flutter. Numerical analysis corresponding to the wind tunnel test are performed by Euler / Navier-Stokes code. In addition to the time domain simulation, linearlized generalized aerodynamics, eigen value analysis using harmonic balance method are mentioned in this paper.

2 WING MODEL AND WIND TUNNEL TEST

The wing model (Figure 1) and wind tunnel test results are described in [1]. Geometry natural, mode, and some results are depicted in Figure 2 - Figure 5 and Table 1. LCOs were observed under the flow condition as shown in Figure 4. The test was held in blow down wind tunnel, which can operate in Mach or total pressure sweep mode. LCO occurred as total pressure, that is Equivalent Air Speed (EAS), increased. Furthermore, the EAS increased keeping LCO, the amplitude suddenly became large (Figure 5). Therefore, two types of LCO was observed in the test. After large amplitude LCO occurred, the wind tunnel operation was stopped immediately.

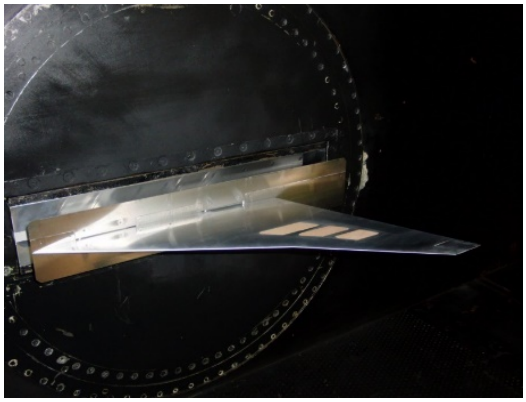

Figure 1: Wing model

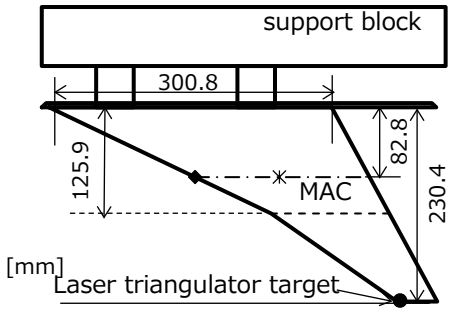

Figure 2: Geometry of the model

Table 1: Natural frequencies

#	mode	FEM Hz	GVT Hz
1	1st bending	65.7	64. 1
2	2nd bending	186.4	186.6
3	1st torsion	352.0	360.8
4	3rd bending	397.0	416.8

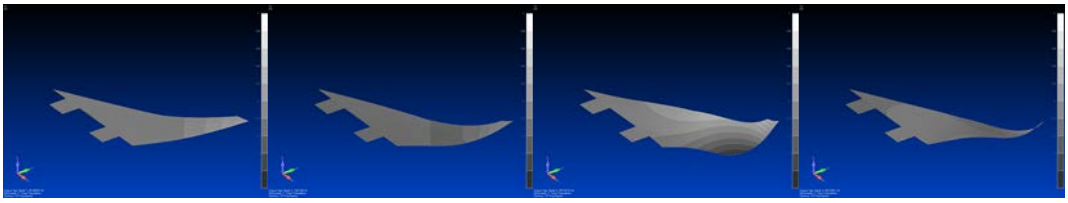

mode 1 mode 2 mode 3 mode 4

Figure 3: Mode shapes by FEM

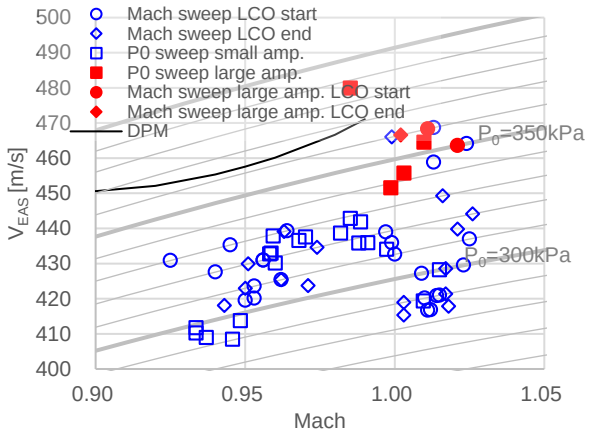

Figure 4: LCO observed in the wind tunnel test

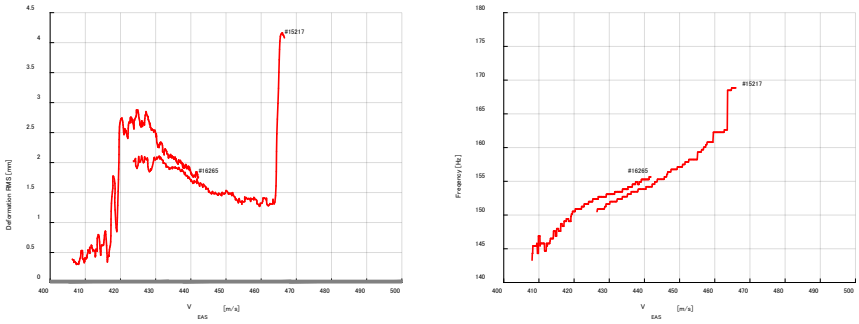

Figure 5: LCO amplitude variation in EAS changes at Mach 1.01.

3 NUMERICAL ANALYSIS

3.1 Linear analysis

Figure 6 shows flutter boundary estimated by Doublet Point Method (DPM) which is based on a lifting surface theory. 8 modes are considered and p-k method was used for the eigen value analysis. The natural mode of splitter plate at the root was omitted. The first and the second flutter modes are hump mode which would be stabilized again as EAS increases over destabilized speed. Symmetric flow in span direction at the splitter plate was supposed in the DPM analysis. FEM was modified by GVT in eigen mode frequencies. At least 4 modes are necessary to get unstable results.

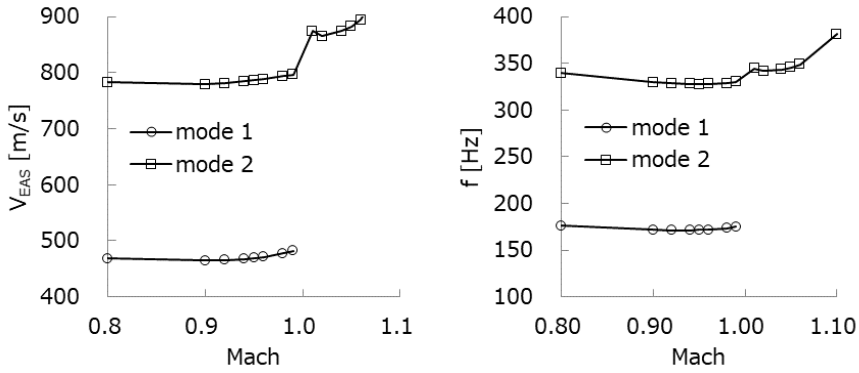

Figure 6: Flutter speed (left) and frequency (right) estimated by DPM.

3.2 Nonlinear analysis

3.2.1 Euler / Navire-stokes code

The numerical analysis was performed by NATAS which is the code developed by JAXA. Summary of the code descriptions is as follows.

flow_solver	MFGS
fluxtype	non-MUSCL
turbulent_model	Spalart-Allmaras
grid	

Euler	structured multiblock grid	18 blocks	node 2.8 mil. points
NS	structured multiblock grid	18 blocks	node 6.9 mil. points

Pressure distributions are shown in Figure 7 and results of the time domain simulation are shown in Figure 8 - Figure 11. Loss factor, frequency and amplitude are estimated from the time history of the first eigenmode response. Positive loss factor means positive damping, which should be damped to the zero amplitude. In some cases, the computations have not been conversed enough to remain a certain amplitude. The conditions where loss factor is zero and the amplitude is non-zero value mean those are in Limit Cycle Oscillation. Negative loss factor means the amplitude still increases. Although different initial speed of the first mode was tried in some cases, no different equivalent condition was reached. Two stage amplitude of LCO in VEAS direction is not appeared in numerical results as observed in the wind tunnel test. LCO amplitude observed in the test is shown in Figure 11 for a reference. It is the amplitude at the measured point, which is not the first mode amplitude. Both viscous and non-viscous simulation reached to LCO condition. Both seem to be corresponded to the large amplitude LCO in the test. No small amplitude LCO was observed in the numerical simulations. Figure 12 shows the first and the second mode generalized aerodynamics (GA) in relation with the modal velocity during NS simulation with two different initial conditions. Higher mode GA shows nonlinearity as the amplitude become large.

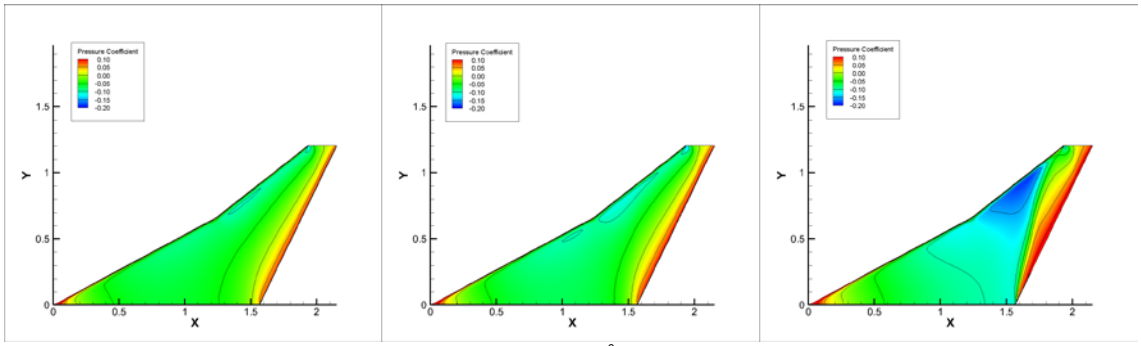

Figure 7: Cp distribution by Euler analysis at $\alpha = 0^{\circ}$, Mach 0.90 (left), 0.95 (center), 0.99 (right)

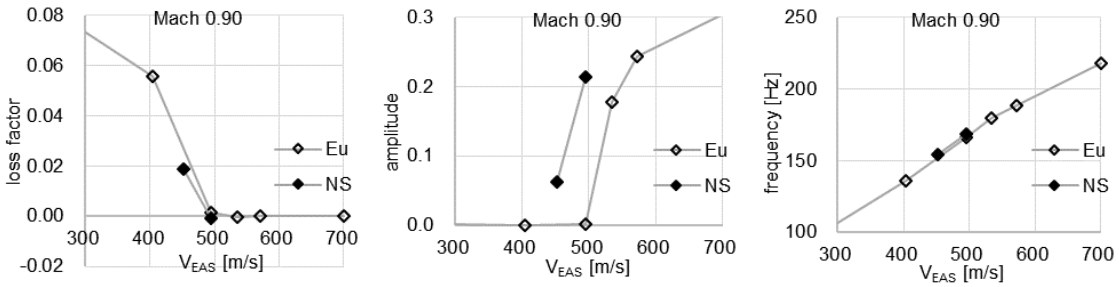

Figure 8: Euler / NS results at Mach 0.90.

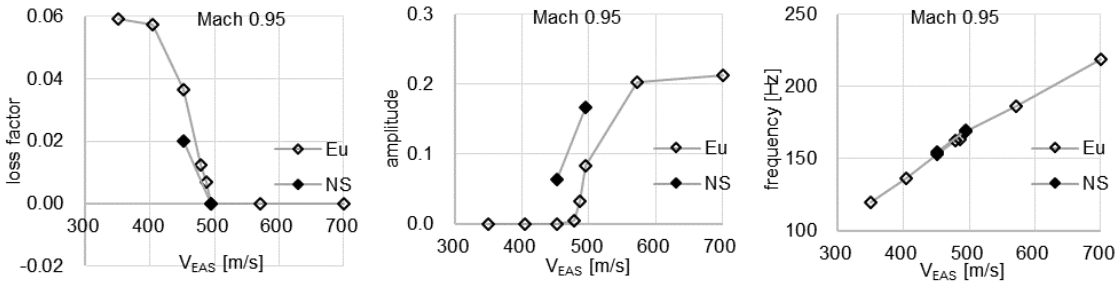

Figure 9: Mach 0.95

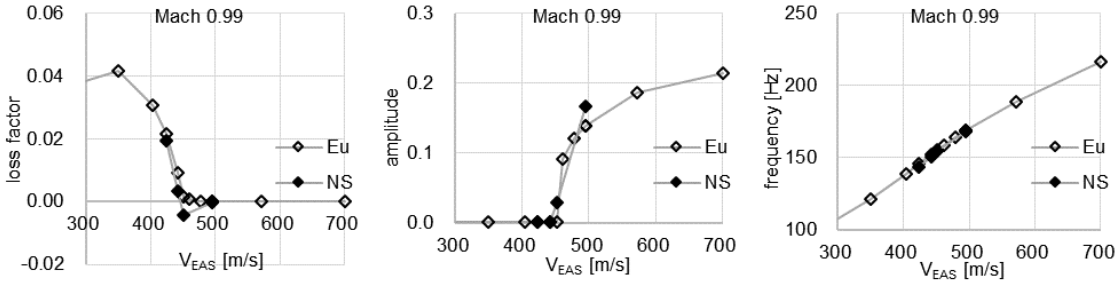

Figure 10: Mach 0.99

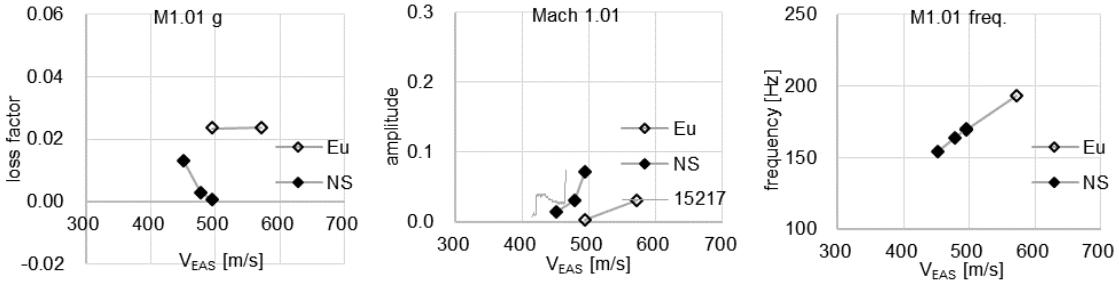

Figure 11: Mach 1.01

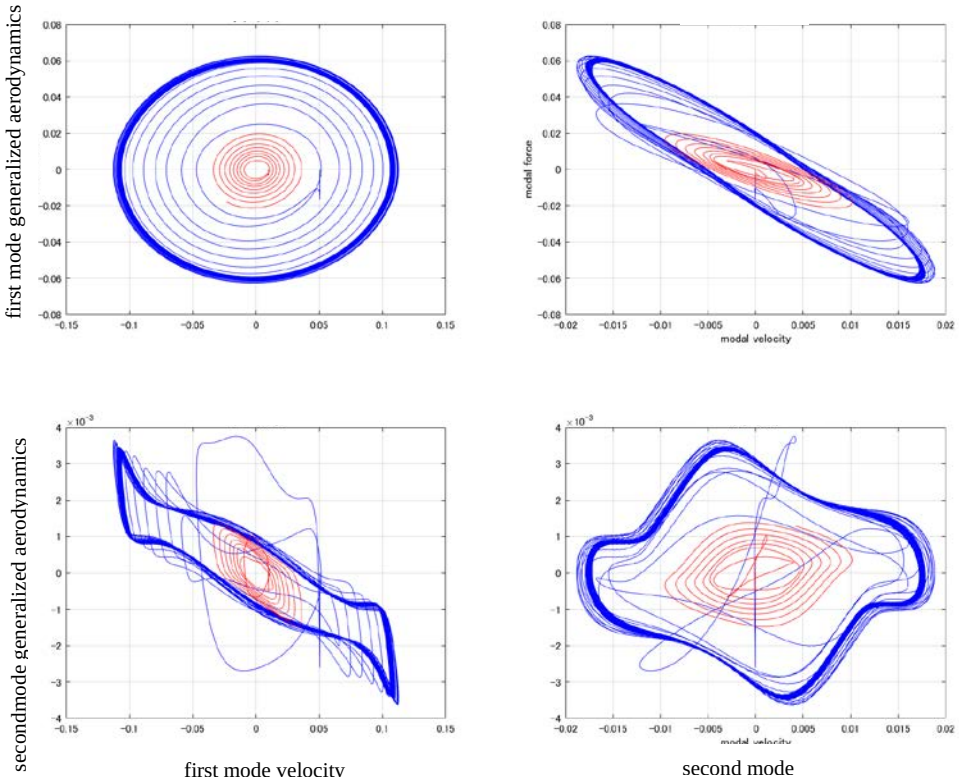

Figure 12: First and second mode GA vs. modal velocity at Mach 0.99 Veas=495m/s by NS analysis

3.2.2 Generalized aerodynamics

Generalized aerodynamics for each natural mode are estimated by the Euler code. Simulation for forced sinusoidal oscillation of the natural mode are performed first, then the time history of the generalized aerodynamics multiplied by the forced sinusoidal signal are integrated and normalized by the amplitude to obtain the coefficient of the Fourier series. Magnitude and phase are shown in Figure 13 for different amplitude with DPM results. No static deformation is

considered in Figure 13 because the wing model has symmetric profile and zero incidence is supposed.

Figure 14 shows the flutter equivalent air speed estimated by the generalized aerodynamics. “Euler pk” in the figure are the results of the p-k method with the first harmonic component of the generalized aerodynamics by the Euler analysis. The flutter speed increases as the amplitude increases. This chart can be recognized as a bifurcation diagram which shows the amplitude of the LCO against the equivalent air speed. Higher speed than flutter is unstable, which means amplitude must be increased. Lower speed than flutter is vice versa. Therefore, the line which has positive inclination gives the equivalent condition at that speed. In this manner, LCO amplitude can be estimated 0.10 at $V_{EAS} \cong 500$ m/s. It is comparable to the time domain simulation result which is 0.14 as in Figure 10. It contains the error caused by super-impose effect, higher harmonic component, etc., comes from the nonlinearity of the aerodynamics.

The harmonic balance method[4] can estimate flutter speed by eigen value analysis considering nonlinearity. In this method a relation between amplitude and flutter speed can be estimated to have a bifurcation diagram. Although the original method needs numerical code solving in frequency domain, it was performed by time domain analysis in this paper. The method is as follows.

Definition of the equation.

The flutter equation is

$$M\ddot{q} + C\dot{q} + Kq = F \tag{1}$$

where M, C, K, F, q are generalized mass, damping, stiffness matrices and aerodynamics, coordinate vectors. It is supposed that the LCO can be expressed as Fourier series expansion as $q = \sum_{\lambda=0}^{n} q_\lambda e^{i\lambda\omega t}$. It is substituted into the equation and generalized aerodynamics is expanded as $F = \sum_{\lambda=0}^{n} \frac{\partial F}{\partial q_\lambda} q_\lambda e^{i\lambda\omega t}$. In each order of the harmonic component λ, following equation is derived.

$$(-\lambda^2\omega^2 M + i\lambda\omega C + K)q_\lambda = \frac{\partial F}{\partial q_\lambda} q_\lambda \tag{2}$$

It can be expressed as

$$(A_R + iA_I)q_\lambda = 0 \tag{3}$$

where $A_{\mathrm{R}} = -\lambda^2\omega^2 M + K - \left(\frac{\partial F}{\partial q_\lambda}\right)_{\mathrm{R}}$, $A_{\mathrm{I}} = \lambda\omega C - \left(\frac{\partial F}{\partial q_\lambda}\right)_{\mathrm{I}}$ and $\frac{\partial F}{\partial q_\lambda} = \left(\frac{\partial F}{\partial q_\lambda}\right)_{\mathrm{R}} + i\left(\frac{\partial F}{\partial q_\lambda}\right)_{\mathrm{I}}$. In this paper, only the first harmonic component is considered and mean condition q_0 is fixed zero vector, because the wing has symmetric profiled and only the case of zero incidence is considered.

Solving equation (3)

Equation (3) is nondimensionalized by reference mass m_r, reference length c, reference time $t_r = c/U_\infty$, where U_∞ is a true air speed of the uniform flow. It results

$$(\bar{A}_R + i\bar{A}_I)\bar{q}_\lambda = 0 \tag{4}$$

where $\bar{A}_R = -\lambda^2 k^2 \bar{M} + \bar{K} - \frac{1}{2\pi\mu}\left(\frac{\partial Q}{\partial \bar{q}_\lambda}\right)_{\mathrm{R}}$, $\bar{A}_I = \lambda k \bar{C} - \frac{1}{2\pi\mu}\left(\frac{\partial Q}{\partial \bar{q}_\lambda}\right)_{\mathrm{I}}$, $k = \omega c/U_\infty$, $\mu = \frac{m_r}{\pi\rho c^3}$. Considering the *m*-th order generalized coordinate, 2*m* equations are derived on each harmonic component. As for the first harmonic component $\bar{q}_1$, the first natural mode is fixed as $\bar{q}_1^1 = \bar{q}_{1,R}^1 + i\bar{q}_{1,I}^1 = \bar{q}_{1,R}^1$, which means the amplitude of the first natural mode is given. The equation can be solved for the rest of the natural mode $\bar{q}_1^\xi = \bar{q}_{1,R}^\xi + i\bar{q}_{1,I}^\xi$, reduced frequency k and mass ratio μ. It is solved by the Newton - Raphson (NR) method from the initial value to obtain converged solution. Although the aerodynamics is obtained by the simulation of the forced oscillation of the LCO mode expressed by the combination of the natural modes, linear aerodynamics can be applied for the initial condition. Once the eigen vector and k, μ are obtained, forced oscillation simulation is performed with the eigen vector with reduced frequency k at mass ratio μ. Generalized aerodynamics for each natural mode $\bar{f}_\xi(t)$ is stored for estimating the complex Fourier series coefficient. Complex Fourier series expansion is

$$\bar{f}_\xi(t) = \sum_{\lambda=-\infty}^{\infty} c_{\xi,\lambda} e^{i\lambda t} \tag{5}$$

and Fourier coefficient is

$$c_{\xi,\lambda} = \frac{1}{2\pi}\int_{-\pi}^{\pi} \bar{f}_\xi(t)\, e^{-i\lambda t} \tag{6}$$

In the present research, five cycles simulation was performed, and last cycle was used for Fourier integration. Fourier coefficients are separated in real and imaginary part and are normalized by the first natural mode amplitude $|\bar{q}_1^1|$, resulting in as follows.

$$(Q_{\xi,\lambda})_R = \frac{c_{\xi,\lambda} + c_{\xi,-\lambda}}{2|\bar{q}_1^1|},\ (Q_{\xi,\lambda})_I = \frac{c_{\xi,\lambda} - c_{\xi,-\lambda}}{2|\bar{q}_1^1|} \tag{7}$$

$$\bar{f}_\xi(t) = |\bar{q}_1^1|\left\{\frac{c_{\xi,0}}{|\bar{q}_1^1|} + \sum_{\lambda=1}^{\infty}\left((Q_{\xi,\lambda})_R + i(Q_{\xi,\lambda})_I\right)e^{i\lambda t}\right\} \tag{8}$$

In equation (4), $\bar{f}_\xi(t)$ is treated as the function of the first natural mode only.

$$\bar{A}_R = -\lambda^2 k^2 \bar{M} + \bar{K} - \frac{1}{2\pi\mu}\begin{bmatrix} (Q_{1,\lambda})_R & 0 & \cdots & 0 \\ \vdots & & & \vdots \\ (Q_{\xi,\lambda})_R & 0 & & 0 \\ \vdots & & & \vdots \\ (Q_{m,\lambda})_R & 0 & \cdots & 0 \end{bmatrix} \tag{9}$$

$$\bar{A}_I = \lambda k \bar{C} - \frac{1}{2\pi\mu}\begin{bmatrix} (Q_{1,\lambda})_I & 0 & \cdots & 0 \\ \vdots & & & \vdots \\ (Q_{\xi,\lambda})_I & 0 & & 0 \\ \vdots & & & \vdots \\ (Q_{m,\lambda})_I & 0 & \cdots & 0 \end{bmatrix} \tag{10}$$

The first natural mode is fixed in equation (4), therefore derivative for Newton-Raphson (NR) iteration is independent to the aerodynamics. It makes difficult in acquiring converged result. As shown in Figure 15, variation of flutter speed and reduced frequency is so large in the iteration. To avoid this difficulty, equation (4) is reconstructed as follows.

$$(S + \mathcal{F} + \mathcal{F}')(\bar{q}_\lambda^{[\eta]} + \Delta\bar{q}_\lambda) = 0$$

where S is structural part of the matrix, $\mathcal{F}$ is the aerodynamics previously mentioned, $\mathcal{F}'$ is gradient of the aerodynamics, $\bar{q}_\lambda^{[\eta]}$ is eigen vector solution at η step iteration, $\Delta\bar{q}_\lambda$ is difference to the $\eta + 1$ step solution. Although precise $\mathcal{F}'$ is preferable, generalized aerodynamics obtained by the forced oscillation simulation with Euler code as shown in Figure 13 is adopted. Consequently, the convergence in the NR iteration become much better as shown in Figure 16. Figure 17 shows a difference of GA and eigen vector between the beginning and converged value in NR iteration. Furthermore, eliminating the overshooting in the iteration, damping factor for convergence is applied. $\eta + 1$ step variable $x^{[\eta+1]}$ is changed as

$$x^{[\eta+1]} \leftarrow x^{[\eta]} + \varsigma(x^{[\eta+1]} - x^{[\eta]})$$

Figure 18 and Figure 19 shows the results by this manner with $\varsigma = 0.5$.

In Figure 14 flutter speed estimated by NR method is shown. Flutter speed is slightly lower than the p-k method in this case.

Flutter boundary changes in Mach variation is shown in Figure 20. The amplitude of the first natural mode is 0.05 for NR method. 8 modes for Euler simulation and 4 modes for eigen value analysis are considered unless explicitly indicated. As previously mentioned, small amplitude LCO can not be captured by Euler simulation, therefore the boundary in Figure 20 means for flutter or large amplitude LCO. Both simulation and eigenvalue analysis by Euler code shows LCO speed reduction close to sonic speed, while DPM boundary shows slightly increase. LCO appears in Euler simulation at lower EAS estimated by eigen value analysis with Euler code. By DPM analysis, number of modes considered influence on the flutter speed close to Mach one. Eigen value analysis with Euler code only consider 4 modes while the 8 modes are considered in the simulation, therefore it might cause the difference of the LCO boundary.

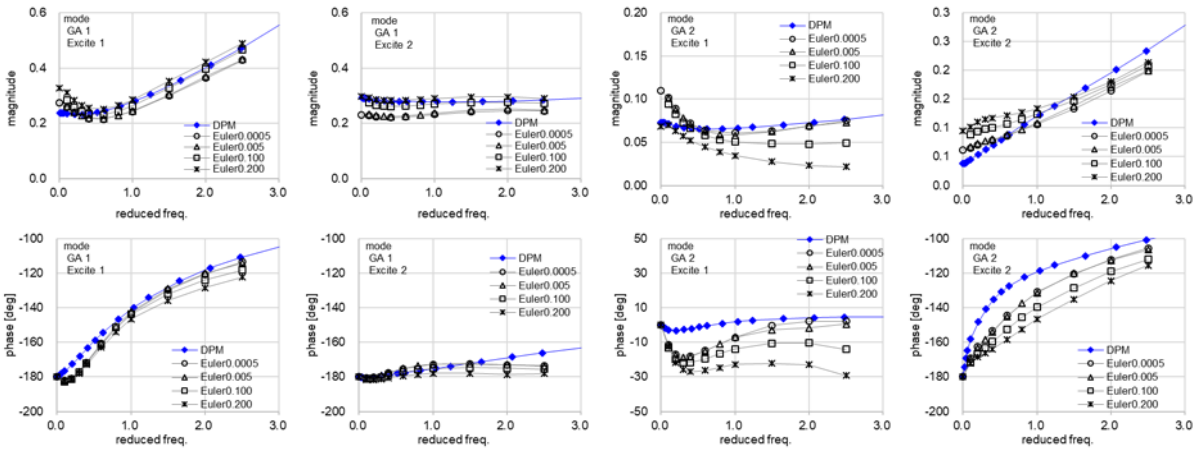

Figure 13: Generalized aerodynamics (mode 1 and 2 Excited by mode 1, 2 at Mach 0.99)

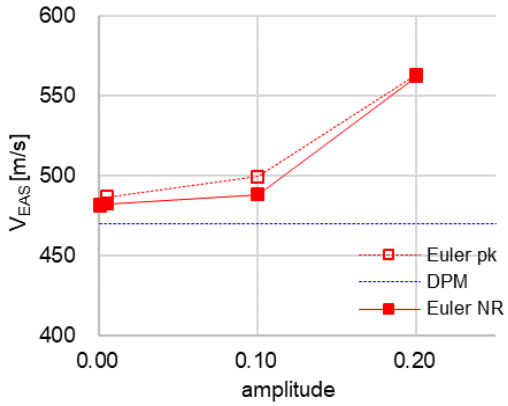

Figure 14: Amplitude effect on the flutter equivalent air speed at Mach 0.99.

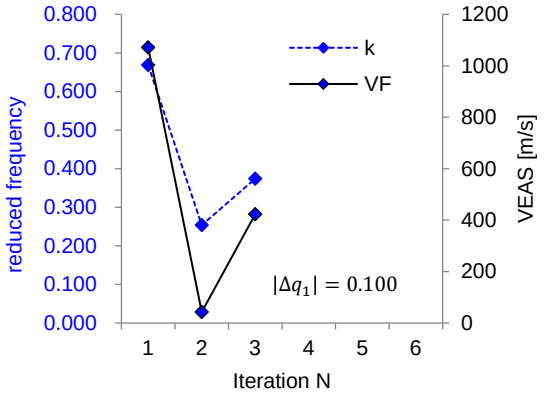

Figure 15: Flutter speed and reduced frequency variation in NR method iteration. Mach 0.99, first mode amplitude is $|\Delta q_1| = 0.100$. GA is independent in the iteration

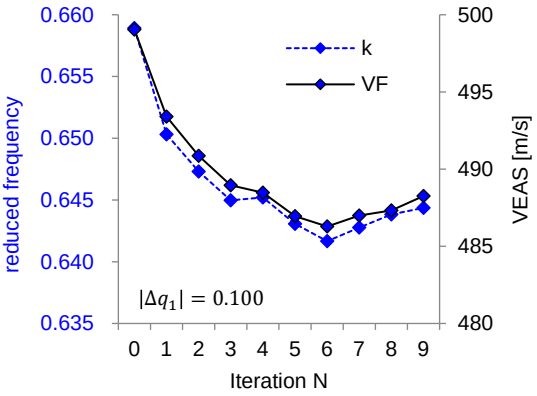

Figure 16: Flutter speed and reduced frequency variation in NR method iteration. Mach 0.99, first mode amplitude is $|\Delta q_1| = 0.100$. GA is considered for perturbed part

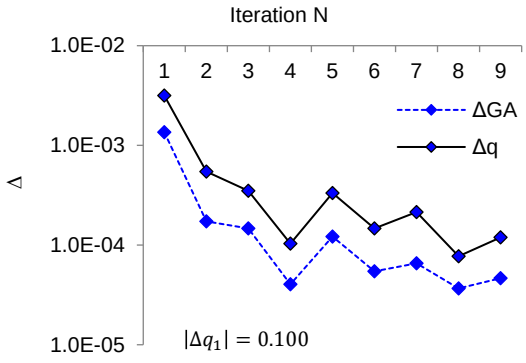

Figure 17: Difference of GA and eigen vector in NR iteration corresponding to Figure 16.

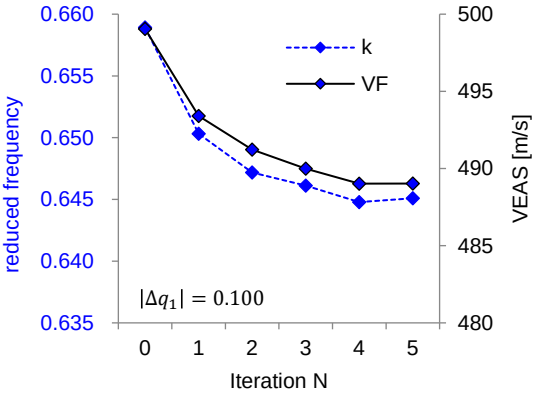

Figure 18: Flutter speed and reduced frequency variation in NR method iteration. Mach 0.99, first mode amplitude is $|\Delta q_1| = 0.100$. Considering converged factor.

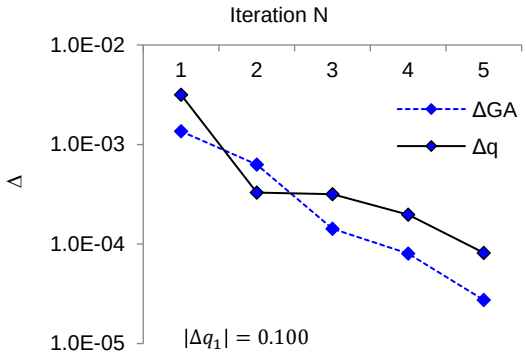

Figure 19: Difference of GA and eigen vector in NR iteration corresponding to Figure 18.

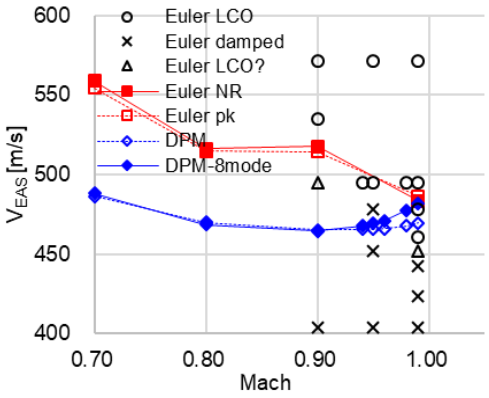

Figure 20: Flutter speed vs. Mach, $|\Delta q_1| = 0.005$ for NR.

4 CONCLUDING REMARKS

Numerical analysis was performed for the wind tunnel test of Super Sonic Transport wing model. Conclusion is as follows.

- Large amplitude LCOs are captured by inviscid numerical simulation, which means flow separation with viscosity is not dominate for the limitation of the oscillation in amplitude.
- Small amplitude LCOs are not observed in the numerical analysis both viscos, inviscid code. We may need more accurate turbulence model to capture it and need more precise test data.
- Generalized aerodynamics of natural mode is calculated by Euler code. Fourier integration of the time history of generalized aerodynamics are performed with different amplitude forced oscillation of the natural modes. GA obtained by different amplitude give the flutter speed change estimated by p-k method.
- Newton-Raphson method using time domain CFD simulation is proposed. The result in flutter speed is close to it estimated by p-k method with linearlized GA.
- Bifurcation diagram was obtained, and it shows comparable LCO amplitude to CFD simulation.

5 REFERENCES

[1] Silva W. A., Florance J. R., Cole S. R. and Scott R. C, “Experimental Steady and Unsteady Aerodynamic and Flutter Results for HSCT Semispan Models”, AIAA-2000-1697, pp.1-11, 2000

[2] Arizono, H., Machida, S., Kikuchi, T., Saitoh, K., Tamayama, M., Nakamichi, J., (2009) Experimental Transonic Flutter Results for Flexible Supersonic Transport Models. JAXA-RR-08-011 (in Japanese)

[3] Saitoh, K., Yoshimoto, N. and Kheirandish, H., “Limit Cycle Oscillation of a Supersonic Transport Model in a Transonic Wind Tunnel Test”, IFASD 2017

[4] Thomas, J.P., Dowell, E.H. and Hall, K.C.: Modeling Viscous Transonic Limit-Cycle Oscillation Behavior Using a Harmonic Balance Approach, J. of Aircraft, 41 (2004), pp.1266–1274.

COPYRIGHT STATEMENT